Laser Chem. 1983, Vol. 2, pp. 229–241
0278–6273/83/0206–0229$12.00/0

Printed in Great Britain

The Spectroscopy of Transition States in $H + H_2$ Reaction, and NaI Photodissociation

H.-J. FOTH, H. R. MAYNE, R. A. POIRIER, J. C. POLANYI and H. H. TELLE

Department of Chemistry, University of Toronto, Toronto, Canada M5S 1A1

(a). We have computed an approximate absorption spectrum for unstable intermediates $H_3^{\neq}$ which constitute the transition states in the fundamental exchange reaction $H + H_2 \rightarrow H_3^{\neq} \rightarrow H_2 + H$. Reaction takes place across the Siegbahn, Liu, Truhlar, Horowitz (SLTH) ground state energy surface, and electronic excitation is to the bound state that correlates with $H^*(2^2P) + H_2$. Features in the spectrum are indicative of the favored turning points for the mean of many classical trajectories across the SLTH surface. (b). Preliminary experimental data are reported which give evidence of emission arising from the transition states of $NaI^{\neq *}$ in the (cw or pulsed) photolysis of $NaI \xrightarrow{222\,nm} NaI^{\neq *} \rightarrow Na^*(3^2P) + I$. The observed transition state emission is compared with a simple calculation.

INTRODUCTION

The dynamics, i.e., the molecular motions, in simple reactions has been studied over the past two decades by "state-to-state chemistry," in which the motions of the reaction intermediate are inferred from the motions of reagents and of newly-formed products. More recently proposals have been made for extending the range of data to include spectroscopic studies of the intermediate configurations themselves. Since in simple reactions the system passes directly through these configurations without lingering as a reaction complex, the new data comprise a spectroscopy of "transition states," i.e., spectroscopy of the range of configurations $ABC^{\neq}$ intermediate between reagents $A + BC$ and products $AB + C$.

The modest number of experiments performed in this area, have been reviewed recently.[1,2] The present paper reports new results on

(a) computed absorption spectra for the transition states $H_3^{\neq}$ in the celebrated exchange reaction $H+H_2 \rightarrow H_2+H$, and (b) measured emission which appears to arise from the transition states $NaI^{\neq *}$ in the photodissociation of NaI to give Na* +I. Both (a) and (b) constitute preliminary studies.

1. COMPUTED ABSORPTION SPECTRA FOR $H_3^{\neq}$

Curiously, discussion of the possibilities for spectroscopy of transition states has not until now encompassed the case of the most fundamental of chemical exchange reactions,

$$H+H_2 \longrightarrow H_3^{\neq} \longrightarrow H_2+H \qquad (1)$$

(here H is (1^2S) and H_2 is $^1\Sigma_g^+$; i.e., both are in their electronic ground states).

The time is opportune for consideration of this case since, recently, Herzberg and co-workers[3] have observed emission spectra due to transitions between the bound electronic states of H_3^*. Some of these downward transitions take place to the $^2A_2''$ excited state. This is the upper state for the electronic absorption spectra of $H_3^{\neq}$ computed below. The $^2A_2''$ state comes from $H^*(2^2P)+H_2(^1\Sigma_g^+)$, where H* is the upper state of the Lyman-α transition at 1216 Å. Consequently the absorption spectra we have calculated for $H_3^{\neq}$ represents a "wing" on the Lyman-α (L_α) absorption line.[4]

For the purposes of the present study, in which the intention is to explore the qualitative features of the spectrum, we have, as in our earlier computations on the emission from transition states $FNaNa^{\neq *}$,[5] assumed that the transition moment is constant. This is a crude assumption in the present case, since the wings further away from the (strongly-allowed) L_α line no longer arise from a perturbed atom but come from a molecular transition which, though allowed for all asymmetric nuclear configurations is disallowed for symmetric configurations (see below). In later work we shall include the effect of changing transition moment.

1.1. $H+H_2$ Calculations

Potential energy surfaces As the ground state potential energy surface for H_3 in these calculations we used the accurate potential due

to Siegbahn, Liu, Truhlar and Horowitz[6-7] (SLTH). A contour plot of this surface for the collinear geometry is shown in Figure 1a.

The collinear excited state H_3^* surface was generated by fitting a rotated Morse[8] function through 11 SCF energies for the $^2\Pi_u$ surface in the $D_{\infty h}$ equilateral collinear symmetry. These single point calculations were performed within the restricted Hartree–Fock formalism using the MONSTERGAUSS(1) program[9] of the University of Toronto. The basis set consisted of a set of 5s3p Gaussians on each hydrogen atom. The $5s3p$ set consists of a standard 31G contracted set augmented with a set of $3sp$ functions ($3s$ and $3p$ with $s = p$). The p-exponents were those of King and Morokuma.[10] In addition three Rydberg functions (also of sp type), with the Gaussian exponent employed by King and Morokuma, were added to the central hydrogen atom. The basis set thus consisted of $5s3p$ functions for each H, together with a $3s3p$ Rydberg set – – for a total of 54 functions.

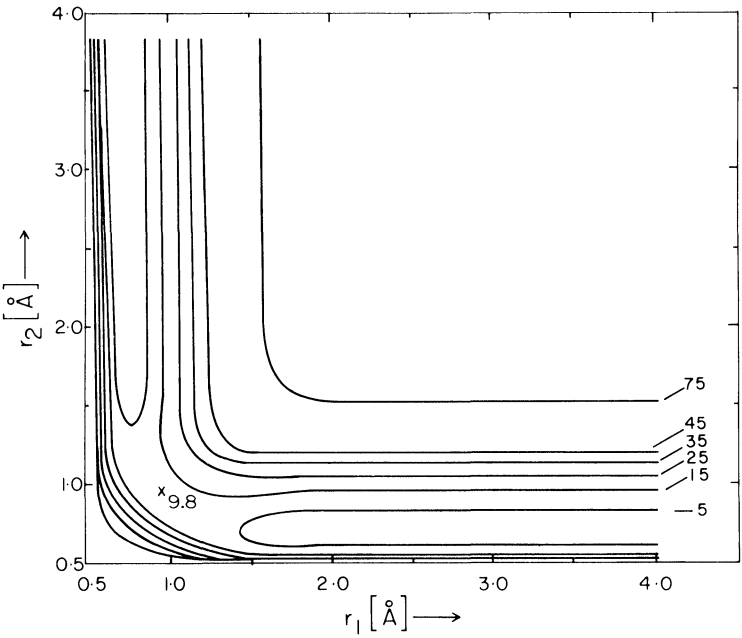

FIGURE 1 (a) Contour plot of the SLTH potential energy surface for ground state $H_3(^1\Sigma_g^+)$ in the collinear configuration. (b) Contour plot of the rotated Morse potential energy surface for the electronically excited state H_3^* ($^2\Pi_u$), in the collinear configuration. The internuclear separations are r_1 and r_2. Contours are labelled in kcal/mol.

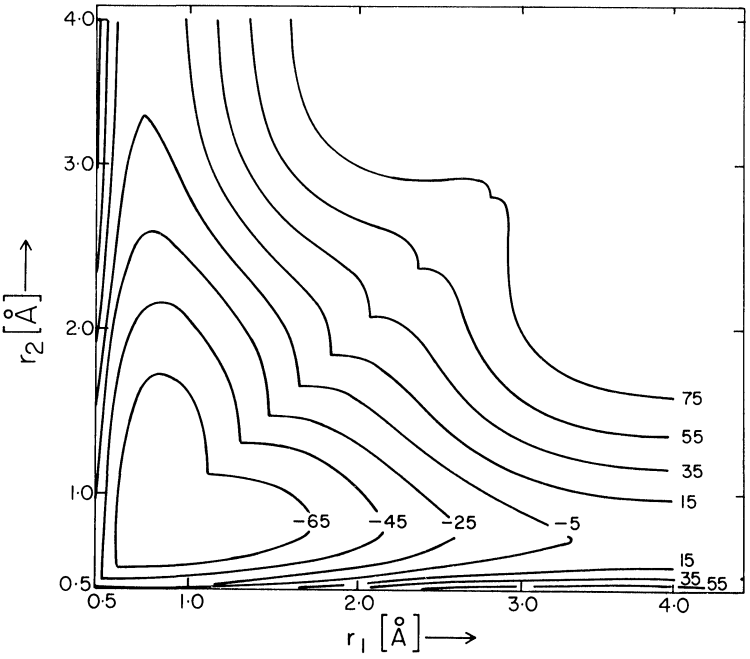

FIGURE 1(b)

A preliminary potential energy surface was generated by swinging a Morse curve about the point $r_1 = r_2 = 4.23$ Å $= r_s$ from the asymptotic H_2 potential through the $D_{\infty h}$ ($r_1 = r_2$) points (this surface will be smoothed in later work). These points were fitted by least squares to Morse parameters, $D^{\neq}$, $r_e^{\neq}$ and $\beta^{\neq}$ (well-depth, equilibrium bond length and force constant, respectively). These constants are given in Table I.

TABLE I
Morse parameters used in rotated Morse potential for H_3^*

	D [kcal/mol]	r_e [Å]	β [Å^{-1}]
H_2 fragment	109.5	0.74	1.95
$\neq$	191.8	0.79	1.13

Progress from $H+H_2$ to $H_3^{\neq}$ was mapped by the variable $\phi = \arctan[(r_s - r_1)/(r_s - r_2)]$. The surface was then formed by a Morse potential at each ϕ, with the Morse parameters given by $v(\phi) = v(0) + (v^{\neq} - v(0))f(\phi)$, where $v = D$, r_e and β. The function $f(\phi)$ was chosen to be a Gaussian; $\exp(-\alpha(\phi - \pi/4)^2)$, with α arbitrarily taken as 10.0 to generate Morse parameters which interpolate between the asymptote and the symmetric configuration.

In addition, in order that the asymptotic diatomic curve be parallel with that of the SLTH (which fits the accurate H_2 points of Kolos and Wolniewicz[11]) a van der Waals term was added, defined as:

$$V^{\text{vdW}}(r_1, r_2) = V^{\text{SLTH}}(r_m, \infty) - V^{\text{Morse}}(r_m, \infty)$$

where r_m is the smaller of r_1, r_2.

The full potential for H_3^* was then given by

$$V^*(r_1, r_2) = V^{\text{Morse}}(r_1, r_2) + V^{\text{vdW}}(r_1, r_2)$$

with

$$V^{\text{Morse}}(r_1, r_2) = D(\phi)X(\phi)(X(\phi) - 2)$$

and

$$X(\phi) = \exp[-\beta(\phi)(r_m - r_e(\phi))]$$

This potential is shown in Figure 1b.

The energy of the photon absorbed at any geometry on the lower surface is the vertical energy difference between the lower and upper potential energy surfaces for that geometry. This difference potential ($= V^* - V^{\text{SLTH}}$) (in frequency units) is shown in Figure 2.

Classical trajectory calculations Collinear classical trajectory calculations were carried out on the lower (SLTH) potential surface. The absorption intensity, $I(\nu)$, was taken to be proportional to the amount of time the trajectory spent at the geometry where the difference potential was ν. The transition moment was assumed to be a constant.

The (r_1, r_2) coordinates were "boxed" into small regions; near the saddle point (for example) the box side-lengths were $dr_1 = 0.005$ Å, $dr_2 = 0.012$ Å. After each integration step (4.2×10^{-17} s), the value of (r_1, r_2) was noted, and the "counter" for the box containing (r_1, r_2) was incremented by one. For each set of initial conditions, several trajectories were run, spanning the vibrational phase of the H_2 diatom.

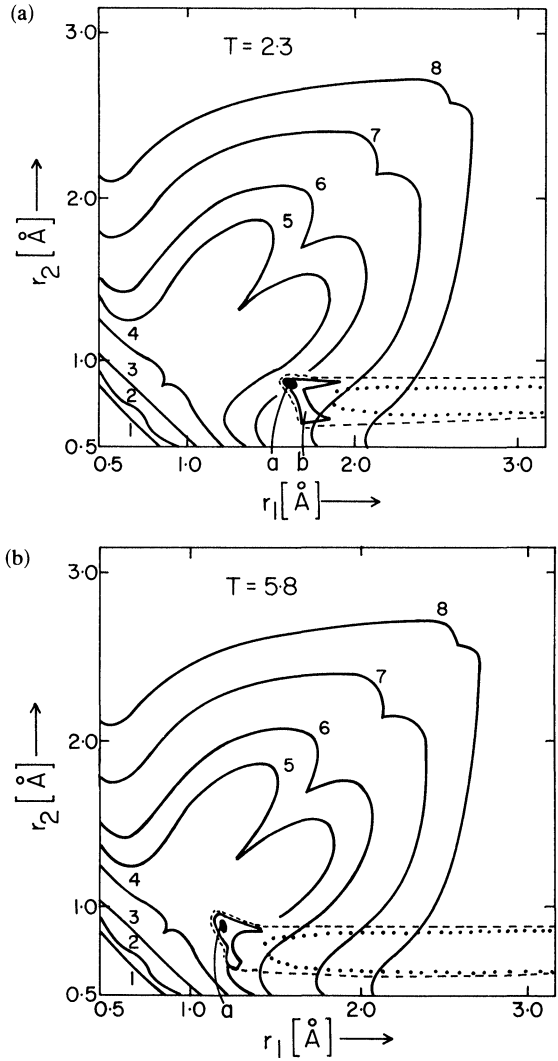

FIGURE 2 Difference potential ($= V^* - V^{\mathrm{SLTH}}$) contour plot for collinear configurations, showing the probability density function for three translational energies. (a) $T = 2.3$ (b) $T = 5.8$ (c) $T = 23$ kcal/mol. The contours are at the following frequencies: $\nu(1) = 38\,000$, $\nu(2) = 41\,000$; $\nu(3) = 46\,000$; $\nu(4) = 50\,000$; $\nu(5) = 53\,000$; $\nu(6) = 56\,000$; $\nu(7) = 62\,000$; $\nu(8) = 68\,000$; (all in cm^{-1}). Probability density plots are normalised to their respective peaks. The density contours at the lower right of Figures 2a and 2b, and across the entire reactive pathway in Figure 2c, show · · · · 0.1; – – – 0.2; —— 0.6; —— 1.0, relative to the peak density.

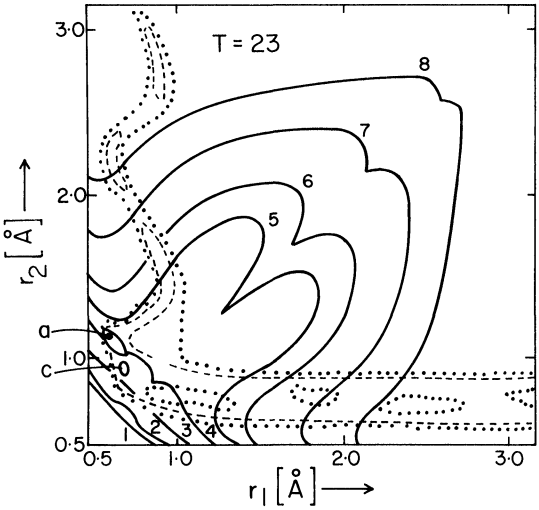

FIGURE 2(c)

After all the trajectories had been run, a cumulative record of box "visits" was available. This was converted into a probability density function by normalising to unit box size. Three examples of such density functions for $H+H_2$ ($v=0$) are given in Figures 2a–c.

By scanning the difference potential as a function of (r_1, r_2), the density was assigned to a frequency, ν. The sum of all densities contributing to an absorption frequency was considered to be the intensity of the absorption spectrum for that ν. Absorption spectra corresponding to the three energies of Figure 2 are given in Figure 3.

1.2. Interpretation of the $H_3^{\neq}$ Spectra

The spectra given in Figure 3 were calculated for collinear reaction $H+H_2 \rightarrow H_2+H$. Since collinear reaction is the preferred geometry, the results should have qualitative validity. As noted above, no account was taken of changing transition moment with internuclear separation. In the real 3D case the electronic transition in absorption is from A' to A''. It is optically allowed except in certain highly symmetrical internuclear separations (D_{3h} for equilateral triangle, or $D_{\infty h}$ for symmetrical collinear). Since the system passes through such configurations, inclusion of a variable transition moment will be

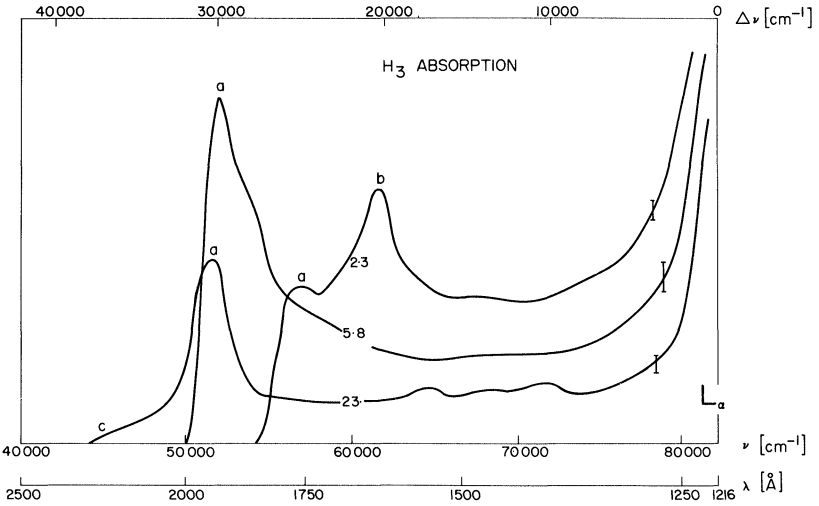

FIGURE 3 Absorption intensity for $H_3 \rightarrow H_3^*$ for translational energies of 2.3, 5.8 and 23 kcal/mol. The ordinate is in arbitrary units. The transition at 1216 Å is the Lyman-α (L_α) line. The scale across the top of the figure gives the displacement of the frequency ($\Delta\nu$) from L_α. Wavelengths (in Å) marked a, b, c correspond to similarly labelled energy-differences (in units of ν, cm^{-1}) in Figure 2.

necessary in a later stage of computation. None of the interesting features discussed below are located at these symmetrical configuration.

Low collision energy; $T = 2.3$ kcal/mol The $T = 2.3$ kcal/mol spectrum in Figure 3 shows a peak at 1760 Å and a second peak at 1610 Å. These features can be understood in terms of the density distribution (averaged over approx. 200 trajectories) on the lower pes of Figure 1a. The density distribution is shown in Figure 2a, superimposed on the difference contours. The trajectories start at the lower right of Figure 1a, and hence 2a, with zero-point vibration $V_0 = 6.3$ kcal/mol, and with $T = 2.3$ kcal/mol carrying the trajectories toward smaller r_1. The pile-up in density at $r_1 \approx 1.7$ Å constitutes the "translational turning point." At this point $T = 2.3$ kcal/mol and some of the $V = 6.3$ kcal/mol has been converted into potential energy. The trajectories subsequently return to the reagent region (large r_1). Before reverting to reagents they oscillate to-and-fro, perpendicular to the entry valley on the properly skewed surface (skewed 30° away

from rectilinear). This oscillation gives rise to vibrational turning points, with the larger density at the outer turning point. This is evident at the points marked *a* and *b* in Figure 2a. They correspond to the peaks labelled *a* and *b* in the 2.3 kcal spectrum shown in Figure 3.

Medium collision energy; $T = 5.8$ kcal/mol The $T = 5.8$ kcal/mol spectrum of Figure 3 exhibits one sharp feature that dominates all others. This is at 1920 Å. It is labelled *a* on the spectrum, and also on the density distribution for trajectories shown in Figure 2b. The absence of two distinguishable spectral peaks corresponding to the vibrational turning points is likely to be due to the fact that at these reagent energies the system is approaching the threshold energy for reaction ($T_0 \approx 7$ kcal/mol^{-1}), and the reagent $T + V$ is to a large extent being channelled into motion along the approach to the col. The turning-point is, therefore, largely a translational turning point.

High collision energy; $T = 23$ kcal/mol In the high collision energy regime of $T = 23$ kcal mol^{-1} reaction is the major pathway. The spectrum of $H_3^{\neq}$ would be expected to show vibrational turning points due to oscillation of the averaged motion across the exit valley. We have not, at the time of writing, identified these. In Figure 3 the $T = 23$ kcal/mol wing-spectrum is labelled as having one identified feature, at *a*. This corresponds to the first turning point of the products in the exit valley, clearly visible in Figure 2c at *a*.

It is the compressed configurations at *c* in Figure 2c that are responsible for the long-wavelength tail at *c* in the spectrum of Figure 3. It is likely that the importance of these compressed configurations (and hence of the spectral features associated with them) will increase as the collision energy is raised still further above threshold, with a resulting diminution in reactive cross-section and increase in the cross reaction for non-reactive inelastic encounters. As already noted this might be difficult to observe spectroscopically in view of the low transition moment in symmetrical configurations for the particular upper electronic state considered here.

It is evident, however, that the spectrum of the transition states of $H_3^{\neq}$ embodies information regarding the dynamics of the reaction $H + H_2 \rightarrow H_2 + H$, that could serve as a valuable supplement to information gleaned from studies of molecular motions in the asymptotic limits of reagent and product.

2. EXPERIMENTAL STUDY OF $NaI^{\neq *}$ EMISSION

Interpretation of the transition state spectra even for the simple reactive system discussed above, will be arduous in view of the three internuclear separations that must be specified. We have, therefore, sought a simpler example which would lend itself to the development of the method.

The example is one which we have discussed from a theoretical standpoint in earlier work.[2] It involves the study of "wing" emission which should accompany the well-known D-line emission following ultraviolet (UV) photodissociation of NaI vapor.[14] This wing, which has not previously been observed, would arise from the emission of transition states $Na^{\neq *}$ *en route* to product;

$$\begin{array}{ccccc} NaI & \xrightarrow{UV} & NaI^{\neq *} & \longrightarrow & Na^*(3^2P)+I \\ & & \downarrow & & \downarrow \\ & & \text{Wing} & & \text{D-line} \end{array}$$

The emission shifted to the blue from the D-line is indicated in terms of the potential-energy curves in Figure 4. The spectrum can be interpreted in terms of a single internuclear separation, consequently the prospects for extracting these potentials from a knowledge of the variations in shape and intensity of the wing emission with excitation wavelength, appear to be good.

In Figure 5 we show the results of a preliminary study of the wing emission. Two sources of UV excitation, both with wavelengths close to 220 nm, were employed. Our earlier experiments made use of a cw source; a Cd/Xe arc lamp followed by a monochromator to select ~ 220 nm. In more recent work we have used an intense pulsed source; the KrCl line of an excimer laser (at 222 nm). Both sets of data are recorded in Figure 5. They are in satisfactory agreement. The observed wing intensity was recorded on a double monochromator by photon counting. The wing can be seen from the figure to be greatly in excess of the natural line-width of the D-line (labelled "Lorentz") or the scattered light (labelled "scat"). The wing emission is roughly $7\times$ greater than that predicted from our approximate calculation;[2] more significantly, however, it is of the correct order-of-magnitude. Note that both calculated and observed wings should exhibit vibrational structure, since this is a free→bound transition. The calculations did not include the effect of vibrational quantisation

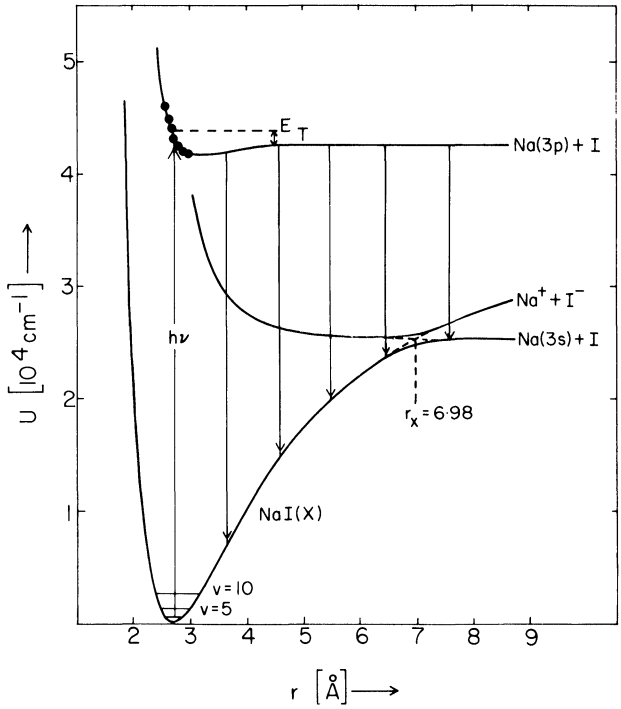

FIGURE 4 Potential-energy curves for NaI in its ground electronic state, and in the repulsive excited state that dissociates to Na* (the upper state of the D-line transition, labelled Na (3*p*)). The excess translational energy in the repulsive excited state (E_T) is relevant to the time available for the transition states, $NaI^{\neq *}$, to emit. The blue-shifted emission in the wings of the D-line due to $NaI^{\neq *}$ is indicated by downward arrows.

in the lower electronic state.[2] The experimental data were recorded with a spectral slit-width of 8.5 Å; too large to show up structure due to the high v states in the lower electronic potential.

Since the transition state $NaI^{\neq *}$ is formed *en route* to Na*+I, increase in the pressure of NaI (P_{NaI}) in the cell should increase the D-line emission and the wing emission by the same factor. This was observed to be the case for a change of P_{NaI} by $\sim 10\times$ in the region 10^{-2}–10^{-1} torr. The finding is significant since broadening of the D-line by collisions of Na* with NaI would cause the wing intensity to increase quadratically with P_{NaI} in contrast to emission from $NaI^{\neq *}$.

These early results indicate that the transition state emission from $NaI^{\neq *}$ *en route* to photodissociation products $Na^* + I$ is readily observable, with an intensity of $10^{-6}\times$ the D-line emission in a bandwidth of 8.5 Å. Further experiments, with varied excitation wavelengths, are under way.

Acknowledgements

It is a pleasure to acknowledge helpful discussions with Dr. N. Sathyamurthy. H.-J.F. thanks the Deutsche Forschungsgemeinschaft for the award of a Fellowship. This work was supported by the Natural Sciences and Engineering Research Council of Canada (NSERC), and in part by the U.S. Air Force Office of Scientific Research and the Occidental Research Corporation of Irvine, California.

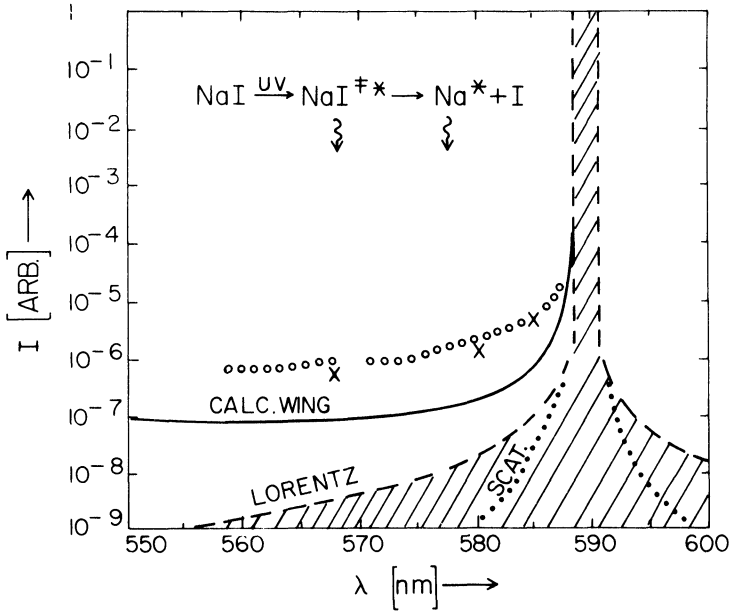

FIGURE 5 The large peak at 589 nm is the D-line. Scattered light, and Lorentz natural line-width of the D-line are indicated as "Scat" and "Lorentz" respectively. The calculated blue-shifted wing intensity was obtained from an approximate calculation based on the potential-energy curves sketched in Figure 4 (see Ref. 2). Points marked × and ○ are experimental; the former come from experiments in which the UV source for excitation of NaI was a cw Cd/Xe arc lamp, the latter come from experiments in which the UV source was the KrCl line from an excimer laser.

References

1. P. R. Brooks, R. F. Curl and T. C. Maguire, *Ber. Bunsenges Phys. Chem.* **86,** 401 (1982).
2. H.-J. Foth, J. C. Polanyi and H. H. Telle, *J. Phys. Chem.* **86,** 5027 (1982).
3. G. Herzberg, *J. Chem. Phys.* **70,** 4806 (1979); I. Dabrowski and G. Herzberg, *Can. J. Phys.* **58,** 1238 (1980).
4. J. C. Polanyi, *Faraday Disc., Chem. Soc.* **67,** 129 (1979).
5. P. A. Arrowsmith, F. E. Bartoszek, S. H. P. Bly, T. Carrington Jr., P. E. Charters and J. C. Polanyi, *J. Chem. Phys.* **73,** 5895 (1980); P. Arrowsmith, S. H. P. Bly, P. E. Charters and J. C. Polanyi, *J. Chem. Phys.* in press (1983).
6. B. Liu, *J. Chem. Phys.* **58,** 1925 (1973); P. Siegbahn and B. Liu, *J. Chem. Phys.* **68,** 2457 (1978).
7. D. G. Truhlar and C. J. Horowitz, *J. Chem. Phys.* **68,** 2466 (1978); **71,** 1514 (*E*) (1979).
8. F. T. Wall and R. N. Porter, *J. Chem. Phys.* **36,** 3256 (1962).
9. MONSTERGRAUSS, M. R. Peterson and R. A. Poirier, Department of Chemistry, University of Toronto, Toronto, Canada M5S 1A1.
10. H. F. King and K. Morokuma, *J. Chem. Phys.* **71,** 3213 (1979).
11. W. Kolos and L. Wolniewicz, *J. Chem. Phys.* **43,** 2429 (1965).
12. C. R. Quick Jr., R. E. Weston Jr., and G. W. Flynn, *Phys. Lett.* **83,** 15 (1981).
13. F. Magnotta, D. J. Nesbitt and S. R. Leone, *Phys. Lett.* **83,** 21 (1981).
14. B. L. Earl, R. R. Herm, S.-M. Lin and C. A. Mims, *J. Chem. Phys.* **56,** 867 (1972); B. L. Earl and R. R. Herm, *J. Chem. Phys.* **60,** 4568 (1974, and earlier references therein).